

# Immune Escape-Related Gene NXT1 as a Potential Prognostic and Therapeutic Target in Hepatocellular Carcinoma

Jia Guo<sup>1,\*</sup> , Xin Tong<sup>#2,3</sup> , Songtao Liu<sup>1</sup> , Feng Liu<sup>4</sup> , Yachao Qu<sup>5</sup> , Ren Li<sup>2</sup> , Xuli Bao<sup>1</sup> 

<sup>1</sup>Hepatology and Cancer Biotherapy Ward, Beijing You'an Hospital, Capital Medical University, Beijing, China

<sup>2</sup>Department of Clinical Laboratory, Tianjin Medical University Cancer Institute and Hospital, National Clinical Research Center for Cancer, Key Laboratory of Cancer Prevention and Therapy, Tianjin's Clinical Research Center for Cancer, Tianjin, China

<sup>3</sup>Department of Clinical Laboratory, Tianjin Stomatological Hospital, Nankai University School of Medicine, Tianjin Key Laboratory of Oral and Maxillofacial Function Reconstruction, Tianjin, China

<sup>4</sup>Department of Head and Neck Surgery, Shanxi Provincial Cancer Hospital/Shanxi Hospital Cancer Hospital of Chinese Academy of Medical Sciences, Taiyuan, China

<sup>5</sup>Department of Respiratory and Critical Care Medicine, Beijing You'an Hospital, Capital Medical University, Beijing, China

**Cite this article as:** Guo J, Tong X, Liu S, et al. Immune escape-related gene NXT1 as a potential prognostic and therapeutic target in hepatocellular carcinoma. *Turk J Gastroenterol*. 2026;37(1):98-112.

## ABSTRACT

**Background/Aims:** Hepatocellular carcinoma (HCC) constitutes approximately 85% of liver cancers. This study aimed to investigate the role of immune escape-related genes (IEGs) in HCC patients and analyze their relationship with prognosis and immunotherapy, thereby providing a reference for further clinical treatment.

**Materials and Methods:** Datasets were collected from The Cancer Genome Atlas (TCGA) and Gene Expression Omnibus databases. Differential expression analysis was conducted to identify differentially expressed IEGs between normal and HCC tissues. Expression, survival, mutational, and immune profiles of a hub gene nuclear transport factor 2 like export factor 1 (NXT1) were evaluated. Validation of NXT1 expression in adjacent normal and HCC tissues was carried out using RT-qPCR and western blot assays. Next, CCK-8, wound healing, and transwell assays were conducted to evaluate the biological function of NXT1 in HCC cell lines.

**Results:** Analysis of the TCGA-LIHC and GSE164359 datasets revealed that NXT1 was notably elevated in HCC tissues compared to adjacent normal tissues, a finding validated through RT-qPCR and western blot assays. Meanwhile, high levels of NXT1 were associated with an unfavorable prognosis of HCC patients. Mutational analysis indicated a higher incidence of TP53 mutations in the NXT1 high-expression group relative to the NXT1 low-expression group. HCC patients with high NXT1 expression demonstrated an increased proportion of M0 macrophages and regulatory T cells (Tregs) and a decreased proportion of M1 macrophages. Furthermore, deficiency of NXT1 significantly suppressed HCC cell viability, migration, and invasion.

**Conclusion:** Collectively, NXT1 may serve as a valuable prognostic marker and a potential therapeutic target for HCC.

**Keywords:** Hepatocellular carcinoma, immune escape, immunotherapy, NXT1

## INTRODUCTION

Hepatocellular carcinoma (HCC), comprising approximately 85% of primary liver cancer (PLC) cases, is the most prevalent type of PLC and is associated with a high rate of mortality.<sup>1</sup> Early HCC can be treated with surgical resection, local percutaneous ablation, and liver transplantation.<sup>2</sup> Unfortunately, many patients are diagnosed in the late stage with poor prognosis.<sup>3</sup> Due to primary and acquired resistance, most advanced HCC patients cannot obtain long-term benefits from systemic treatment.<sup>4</sup>

In recent years, the introduction of immunotherapy into clinical practice has changed the pattern of cancer

treatment and greatly improved the prognosis of cancer patients.<sup>5</sup> While current treatment guidelines for HCC do not recommend immunotherapy for early or intermediate-stage disease, immune checkpoint inhibitors (ICIs) that target the CTLA-4 or PD-1/PD-L1 axis, such as ipilimumab and durvalumab, have emerged as first-line standard therapies for advanced HCC.<sup>6</sup> These agents have shown promising clinical efficacy in patients with advanced HCC.<sup>7</sup> Studies have pointed out that the existence of the immune escape (IE) phenomenon enables tumor cells to escape from immune clearance, thereby reducing the effectiveness of immunotherapy.<sup>8,9</sup> Increasing evidence shows that various cells in the tumor

\*These authors contributed equally to this work.

Corresponding author: Xuli Bao, e-mail: bxli2001@ccmu.edu.cn

Received: April 17, 2025 Revision Requested: May 19, 2025 Last Revision Received: May 19, 2025 Accepted: May 12, 2025

Publication Date: August 25, 2025

DOI: 10.5152/tjg.2025.24193



microenvironment (TME) are involved in the occurrence of tumor IE.<sup>10</sup> Although the mechanism of tumor IE is complex and is still not well understood, it is worth noticing that some scholars have found that liver cancer cells may enhance the ability to escape immune surveillance and attack by low oxygen metabolism, abnormal expression of self-antigens, and occurrence of epithelial-mesenchymal transition.<sup>11,12</sup> Therefore, a comprehensive analysis of immune escape-related genes (IEGs) expression in the TME of HCC helps formulate reasonable treatment plans. In recent years, the extensive application of bioinformatics technology in tumor immunotherapy can help explore the association between tumors and immune cells more deeply. The objective of this study was to comprehensively analyze IEGs expression levels in HCC patients and their relationship with prognosis and immunotherapy, providing a reference for further clinical management.

## MATERIALS AND METHODS

### Data Acquisition

Gene expression profiling data of 374 liver HCC (LIHC) samples and 50 adjacent normal samples were downloaded from The Cancer Genome Atlas (TCGA) database, as well as clinical information of 368 samples of cancerous tissue that possess comprehensive data regarding patient survival, which can be found in Table 1. Additionally, Mutation Annotation Format (MAF) files of 364 liver cancer patients were obtained for further analysis. Furthermore, the International Cancer Genome Consortium-Liver Cancer-RIKEN-Japan (ICGC-LIRI-JP) dataset was downloaded from the International Cancer Genome Consortium (ICGC), which encompassed a cohort of 260 individuals with HCC, out of which survival data was fully available for 231 patients (Table 2). Samples from the TCGA-LIHC and ICGC-LIRI-JP datasets were analyzed using the Illumina HiSeq platform to obtain raw data. Subsequently, STAR software version 2.7.3 (Cold Spring Harbor Laboratory; New York, USA) was employed to align the raw data with the reference genome, allowing for gene expression matrix generation.

### Main Points

- The gene NXT1 is highly expressed in hepatocellular carcinoma samples.
- Hepatocellular carcinoma patients with high expression of NXT1 have a relatively poor prognosis.
- NXT1 plays oncogenic roles in hepatocellular carcinoma.

**Table 1.** Clinicopathological Characteristics of Liver Hepatocellular Carcinoma Patients from The Cancer Genome Atlas Database

		Patients (n = 368)	
Characteristics		n	%
Gender	Female	119	32.3370
	Male	249	67.6630
Age	<61 years (median)	173	47.0109
	≥61 years (median)	195	52.9891
Race	White	183	49.7283
	Black or African American	17	4.6196
	Asian	157	42.6630
	Unknown	10	2.7174
	American	1	0.2717
Survival time	Long (>5 years)	43	11.6848
	Short (<5 years)	325	88.3152
OS status	Dead	131	35.5978
	Alive	237	64.4022
Stage	I	172	46.7391
	II	85	23.0978
	III	83	22.5543
	IV	4	1.0870
	Unknown	24	6.5217
Grade	G1	55	14.9457
	G2	176	47.8261
	G3	120	32.6087
	G4	12	3.2609
	Unknown	5	1.3587
Pathologic T	T1	182	49.4565
	T2	92	25.0000
	T3	78	21.1957
	T4	13	3.5326
	Unknown	3	0.8152

OS, overall survival.

The GSE164359 dataset was also obtained from the Gene Expression Omnibus (GEO) database, which involved a total of 20 primary tumor specimens and 27 recurrent tumor specimens. This dataset was analyzed using the Illumina HiSeq 4000 platform. Next, STAR software (version 2.7.3) was employed to align the raw data with the reference genome, allowing for gene expression matrix generation.

**Table 2.** Clinicopathological Characteristics of Hepatocellular Carcinoma Patients from International Cancer Genome Consortium-Liver Cancer-RIKEN-Japan Database

Characteristics	Patients (n = 231)	
	n	%
Gender	Female	61 26.41
	Male	170 73.59
Age	<69 years (median)	115 49.78
	≥69 years (median)	116 50.22
Survival time	Long (>5 years)	2 0.87
	Short (<5 years)	229 99.13

Besides, 182 IEGs were sorted out according to the published literature (Supplementary Table 1).<sup>13,14</sup>

### Differential Gene Expression and Functional Enrichment Analysis

The study was performed differential expression analysis using the "limma" package in R language (4.1.0),<sup>15</sup> with  $|\log_2\text{FC}| > 0.5$  and  $P\text{-value} < .05$  as a benchmark for filtering differentially expressed genes (DEGs).

Based on DEGs obtained, Gene Ontology (GO, including biological process (BP), molecular function (MF), and cellular component (CC)) terms and Kyoto Encyclopedia of Genes and Genomes (KEGG) pathways analyses were conducted using the "clusterProfiler" package.<sup>16</sup> A  $P\text{-value}$  less than .05 was considered as the significant threshold.

### Survival Analysis

The approach for estimating the overall survival rates over a 10-year period among various groups was facilitated by utilizing the "survival" and "survminer" packages, which are based on the Kaplan-Meier algorithm. Furthermore, the log-rank test was employed to assess the statistical significance of disparities in survival rates among the distinct groups.

### Mutation Analysis

The MAF files of somatic mutations were obtained from the TCGA database, and then they were input into the "maftools" package for analysis and visualization.

### Infiltration Analysis of Immune Cells

The relative abundance of 22 immune cell types within the samples was determined using CIBERSORT.<sup>17</sup> Subsequently, the immune scores of these samples were

quantified by employing the "estimate" package available in R.

### Gene Prioritization and Biomarker Comparison

The analysis focused on the prioritization of genes through the biomarker assessment component of the Tumor Immune Dysfunction and Exclusion (TIDE) framework, involving an examination of the effects of immune checkpoint blockade (ICB) therapy and the phenotypic consequences of gene knockouts as determined by Clustered Regularly Interspaced Short Palindromic Repeats screening. To quantify the influence of gene expression on patient survival within the dataset of ICB-treated patients, Z-scores derived from Cox proportional hazards regression were utilized.

In further analysis, the overall predictive accuracy of treatment response and patient overall survival (OS) was compared across various cancer types with 7 established biomarkers that reflect tumor immune status. These biomarkers included T-cell clonality (T.Clonality), B-cell clonality (B.Clonality), TIDE score, the estimated score for microsatellite instability (MSI), tumor mutation burden (TMB), the expression levels of the cell surface molecule cluster of differentiation 274 (CD274), and the presence of interferon- $\gamma$  (IFNG).

### Clinical Samples

Tumor tissues and adjacent nontumor tissues were obtained from patients with HCC who underwent surgical resection (n = 10) at Shanxi Provincial Cancer Hospital/ Shanxi Hospital Cancer Hospital of Chinese Academy of Medical Sciences. The general clinical information of patients is shown in Supplementary Table 2. This research adhered to the ethical standards outlined in the Declaration of Helsinki and received approval from the Ethics Committee of Shanxi Provincial Cancer Hospital/ Shanxi Hospital Cancer Hospital of Chinese Academy of Medical Sciences (approval no: KY2024010; date: January 6, 2024). Informed written consent was acquired from all participating patients.

### Reverse Transcription Quantitative Real-Time Polymerase Chain Reaction

The TriQuick Reagent (Solarbio) was employed for isolating total RNA. After that, the isolated RNA underwent reverse transcription to synthesize cDNA utilizing an Evo M-MLV kit (Accurate Biology). Subsequently, the SYBR Master

Mix kit (CWBIO) was used for measuring nuclear transport factor 2 like export factor 1 (NXT1) mRNA expression. Glyceraldehyde-3-Phosphate Dehydrogenase (GAPDH) served as an internal control. The primer sequences used for quantitative polymerase chain reaction are listed in Supplementary Table 3.

#### **Western Blot Assay**

Proteins were separated by 10% SDS-PAGE gels, followed by electrotransfer onto polyvinylidene difluoride membranes. The membranes were blocked and then blotted with primary and secondary antibodies. Subsequently, immunoreactive bands were detected by electrochemiluminescence reagents (Beyotime). The primary antibodies used in this study were as follows: anti-NXT1 and anti-GAPDH antibodies were obtained from Proteintech.

#### **Cell Culture and Transfection**

Transformed human liver epithelial-2 (THLE-2) cells (IMMOCELL) were cultured in a complete Bronchial epithelial growth medium. HCCLM3 (Procell) and Huh-7 (Procell) cells were cultured in a Dulbecco's Modified Eagle Medium (DMEM) medium containing 10% FBS and 1% P/S. HepG2 cells were cultured in Minimum Essential Medium (MEM) medium containing 10% FBS and 1% P/S. All cell lines were maintained at 37°C in a humidified atmosphere containing 5% CO<sub>2</sub>.

HCCLM3 cells were transfected with siRNA negative control (siRNA NC), NXT1 siRNA1, NXT1 siRNA2, and NXT1 siRNA3 using the Transfection Kit. The siRNA sequences are summarized in Supplementary Table 4.

#### **Cell Counting Kit-8 Assay**

HCCLM3 cells (5 × 10<sup>3</sup> cells) were seeded into a 96-well plate at 37°C. Next, 10 µL of CCK-8 solution (Beyotime) was added to each well, and cells were then incubated for 2 hours. The absorbance for each well was assessed using a microplate reader at 450 nm.

#### **Wound Healing Assay**

HCCLM3 cells were plated into 12-well plates at 37°C overnight. Next, a scratch was made in the center of each well using a sterilized pipet tip. After 0, 24, or 48 hours of incubation, photographs were taken using a light microscope.

#### **Transwell Assay**

HCCLM3 cells, suspended in a serum-free medium, were seeded into the upper chamber of the Transwell and incubated with a medium containing 10% FBS in the bottom chamber. After 24 hours of incubation, the cells on the bottom side of the filter were stained with 0.1% crystal violet. Images were subsequently obtained using a light microscope. For cell invasion assays, the filter was pre-coated with Matrigel (Corning) before conducting the experiments.

#### **Statistical Analysis**

Data are shown as means ± SDs. The comparison between 2 groups was conducted using the t-test, whereas one-way ANOVA was employed to assess differences among multiple groups. A P-value of less than .05 was deemed significant.

## **RESULTS**

#### **Detection of Differentially Expressed Immune Escape-Related Genes in Hepatocellular Carcinoma**

We conducted a differential analysis of tumor versus normal tissues within the TCGA-LIHC cohort, identifying 11 927 DEGs (Fig. 1). Additionally, a differential analysis was performed between cancer samples *in situ* and recurrent cancer samples using the GSE164359 dataset, identifying 700 DEGs (Fig. 1). A cross-analysis was then performed between these 2 sets of DEGs and 182 IEGs (Supplementary Table 1), resulting in the identification of 7 overlapping genes (Fig. 1). Notably, these 7 genes exhibited high expression levels in the tumor samples from the TCGA-LIHC dataset (Fig. 1). The analysis of the functional roles of these 7 genes revealed that they were significantly enriched in 91 GO terms (Fig. 1, Supplementary Table 5), and in 10 KEGG Pathways (Fig. 1, Supplementary Table 6).

Among the 7 genes, NXT1 exhibited increased expression levels in tumor specimens from both TCGA and GEO datasets using the online database TNMplot (Fig. 1). Furthermore, in the GEO database, metastatic samples displayed a significant elevation in NXT1 expression compared to both the tumor and normal tissue samples (Fig. 1). Hence, NXT1 was selected as the target IEG.

#### **The Expression and Survival Analysis of NTX1 in Hepatocellular Carcinoma Patients**

In the TCGA-LIHC dataset, which included 368 samples with comprehensive survival data, the levels of NXT1 expression were assessed across various clinical stages of the disease, ranging from I to IV, using the available clinical

details. The findings revealed that *NXT1* expression varied significantly when comparing stage I to both stage II and stage III, with a progressive rise in expression observed (Fig. 2). In addition, *NXT1* expression was analyzed in different histological grades (G1-G4), revealing significant differences among various group pairings including G1 with G3, G1 with G4, G2 with G3, and G2 with G4, all of which demonstrated increasing expression levels (Fig. 2). Furthermore, the expression of *NXT1* was analyzed in the TNM (Tumor, Node, and Metastasis) staging system (T1-T4), and the results showed significant differences between T1 and T2, as well as between T1 and T3, with an increasing expression level (Fig. 2).

Survival analyses were conducted on HCC datasets from both TCGA-LIHC and ICGC-LIRI-JP, stratifying the samples into high-*NXT1* (*NXT1*<sup>high</sup>) and low-*NXT1* (*NXT1*<sup>low</sup>) groups based on the median expression values of *NXT1* (median value = 8.906890596 for the TCGA-LIHC cohort; median value = 57129 for the ICGC-LIRI-JP cohort). The results showed that individuals in the *NXT1*<sup>high</sup> group had a relatively poor prognosis in comparison to those in the *NXT1*<sup>low</sup> group (Fig. 2).

#### **Variations in Mutation Status Between *NXT1*<sup>high</sup> Group and *NXT1*<sup>low</sup> Group**

To gain insights into the underlying genetic mechanisms that promote the growth and advancement of HCC, somatic mutations, and TMB were analyzed in HCC. Using somatic mutation data from the TCGA-LIHC dataset, differences were observed in TMB levels between the *NXT1*<sup>high</sup> group and the *NXT1*<sup>low</sup> group. The mutation analysis showed that the incidence of *TP53* mutations (37%) was the highest in the *NXT1*<sup>high</sup> group (Fig. 3), while the highest incidence in the *NXT1*<sup>low</sup> group was *CTNNB1* mutations (26%) (Fig. 3). Additionally, significant differences in mutations of 45 genes' mutations between *NXT1*<sup>high</sup> group and *NXT1*<sup>low</sup> group were found ( $P < .05$ , Fig. 3). Among the 10 tumor-related pathways examined, the fraction of samples affected by mutations in genes from the *TP53* pathway was higher in *NXT1*<sup>high</sup> group (Fig. 3) compared to *NXT1*<sup>low</sup> group (Fig. 3).

#### **The Relationship Between *NXT1* and Chemokines/Chemokine Receptors**

Chemokines and their receptors are recognized for their significant contributions to the pathology of cancer progression and metastasis. A correlation analysis was conducted between *NXT1* and 41 chemokines as well as 18 chemokine receptors. Based on the criterion

of  $P < .05$  and  $|\text{correlation}| > 0.3$ , significant positive correlations were found between *NXT1* and the chemokines *CCL20*, *CCL26*, *XCL1*, *CXCL3*, and *CXCL5* (Fig. 4). Additionally, *NXT1* also showed significant positive correlations with the chemokine receptors *CCR10* and *CXCR4* (Fig. 4).

#### **Immune Landscapes of High and Low *NXT1* Expression Groups**

Leveraging the CIBERSORT analytical tool, the proportional presence of 22 distinct immune cell populations within HCC samples obtained from the TCGA dataset was determined (Fig. 5). Infiltration ratios of 12 types of immune cells (naive B cells, memory B cells, plasma cells, naive CD4 T cells, follicular helper T cells (Tfh), regulatory T cells (Tregs), resting natural killer (NK) cells, monocytes, macrophages M0, macrophages M1, resting mast cells, neutrophils) exhibited substantial disparities when comparing the *NXT1*<sup>high</sup> and *NXT1*<sup>low</sup> groups (Fig. 5). Additional examination of the relationship between *NXT1* expression levels and the 12 immune cells that showed significant differences revealed a substantial positive association between *NXT1* and Tregs, as well as Tfh (P-value  $< .05$ ) (Fig. 5), and a significant negative correlation with resting mast cells (P-value  $< .05$ ) (Fig. 5).

Moreover, it was found that the ImmuneScore was significantly elevated in the *NXT1*<sup>high</sup> group compared to the *NXT1*<sup>low</sup> group, suggesting that *NXT1* may be a viable target for immunotherapeutic approaches; whereas ESTIMATEScore, TumorPurity, and StromalScore did not exhibit any significant variance between the *NXT1*<sup>high</sup> and *NXT1*<sup>low</sup> groups (Fig. 5). Collectively, these findings indicate a distinct immune landscape between the *NXT1*<sup>high</sup> and *NXT1*<sup>low</sup> groups, which indirectly supports the potential impact of *NXT1* on the tumor immune microenvironment in HCC.

#### ***NXT1* was Valuable in Hepatocellular Carcinoma Immunotherapy**

To further determine *NXT1*'s value on immunotherapy, expression levels of 9 immune checkpoints *PDCD1* (PD-1), *CTLA4*, *TIGIT*, *CD274* (PDL-1), *PDCD1LG2* (PDL-2), *IDO1*, *CD80*, *CD86*, and *LAG3* were analyzed between the *NXT1*<sup>high</sup> group and the *NXT1*<sup>low</sup> group. The findings revealed that the levels of expression for 8 immune checkpoints—*PDCD1* (PD-1), *CTLA4*, *PDCD1LG2* (PDL-2), *CD80*, *CD86*, *LAG3*, *TIGIT*, and *IDO1*—were significantly higher in the *NXT1*<sup>high</sup> group compared to *NXT1*<sup>low</sup> group (Fig. 6).

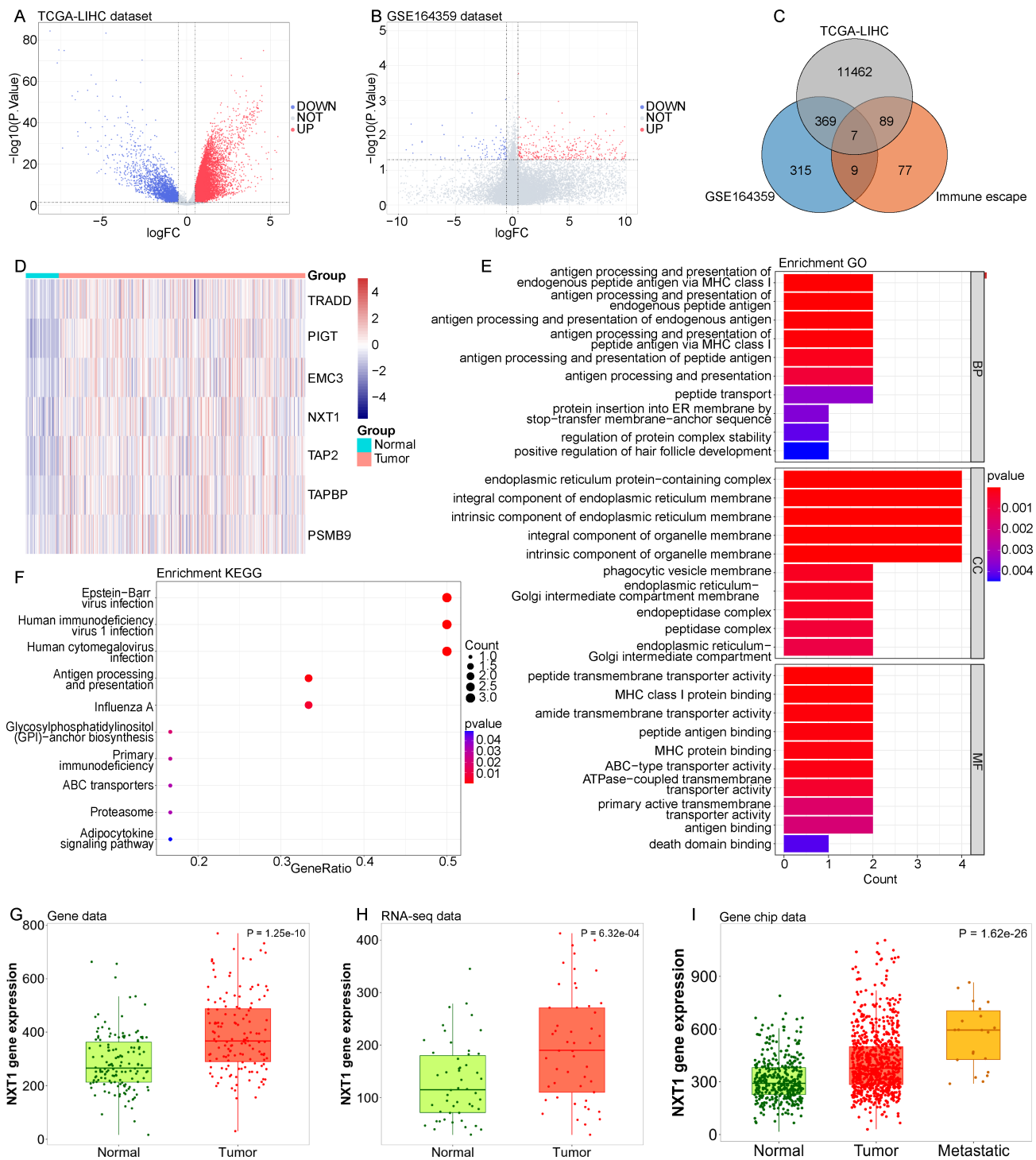


**Figure 1.** Identification of immune escape-related genes in hepatocellular carcinoma. (A, B) Differential gene expression between tumor samples and normal samples in TCGA-LIHC and GSE164359 datasets. (C) Venn diagram demonstrates the intersections of genes among TCGA-LIHC data, GSE164359 data, and 182 IEGs. (D) Heatmap of the expression of 7 intersection genes in normal and LIHC tissues in the TCGA-LIHC dataset. (E, F) GO and KEGG enrichment analysis of these 7 intersection genes. Top 10 significantly enriched GO terms (BP, CC, MF) and KEGG pathways. (G, H) NXT1 expression in normal and HCC tissue was analyzed using the TNMplot database from gene data and RNA-seq data. (I) NXT1 expression in normal, HCC tissue, and metastatic tissue were analyzed using the TNMplot database from gene chip data.

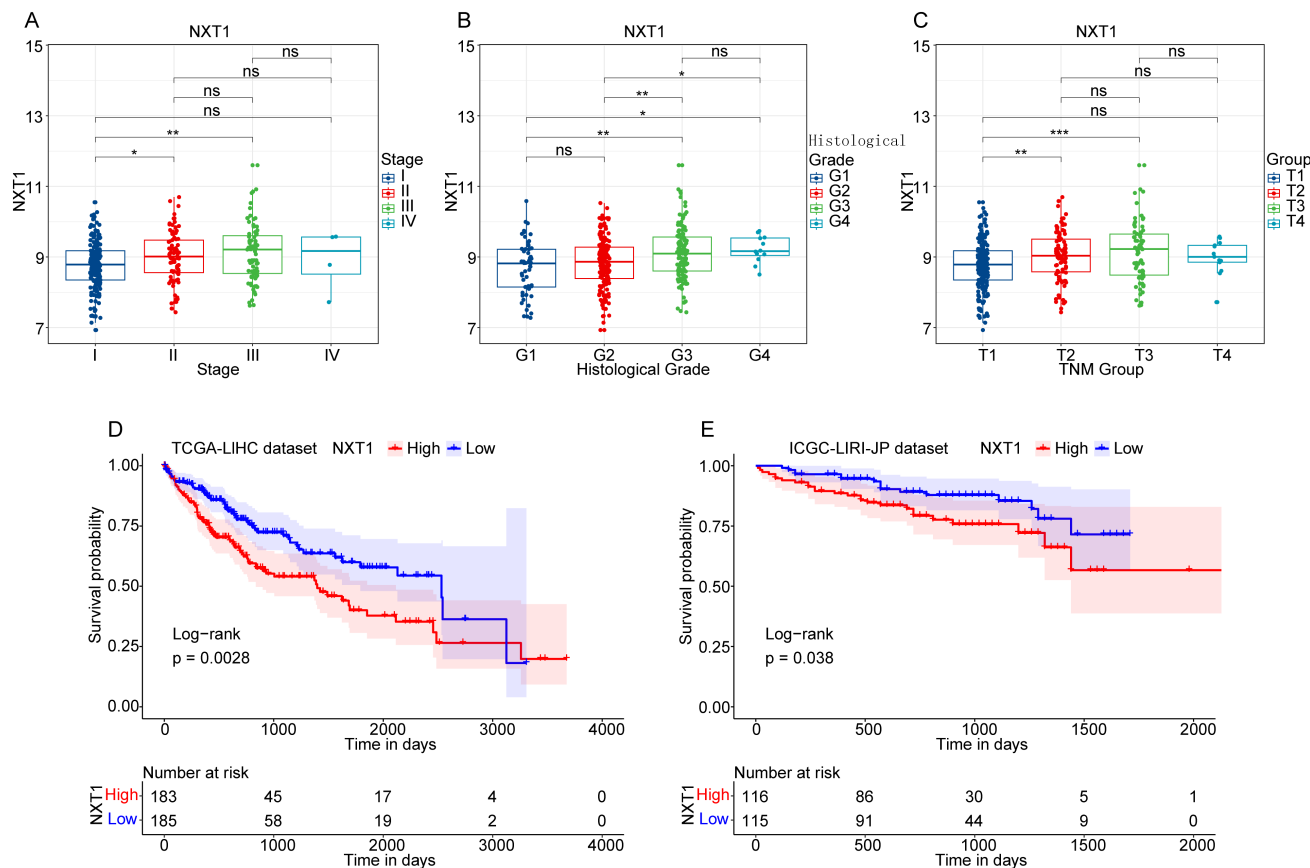


**Figure 2.** The expression and survival analysis of NXT1 in hepatocellular carcinoma patients. (A) The expression of NXT1 in HCC patients at different clinical stages (I, II, III, IV) in the TCGA-LIHC dataset. (B) The expression of NXT1 in HCC patients at different histological grades (G1-G4) in the TCGA-LIHC dataset. (C) The expression of NXT1 in HCC patients at the TNM staging system (T1-T4) in the TCGA-LIHC dataset. (D-E) KM survival analysis between the NXT1<sup>high</sup> group and the NXT1<sup>low</sup> group in TCGA-LIHC and ICGC-LIRI-JP datasets.

Additionally, NXT1 was compared with some standardized biomarkers and evaluated the prognostic value. Among the 25 ICB datasets, it was found that NXT1 alone had an area under the receiver-operating characteristic curve (AUC) of  $\geq 0.5$  in 9 of the 25 ICB sub-cohorts, indicating a more robust predictive capacity compared to TMB (8) and B. Clonality (7), but lower than TIDE score, MSI score, CD27A, IFNG, CD8, T.Clonality, and Merck18 (Fig. 6). In the Miao2018\_ICB dataset, which included immunotherapy clinical response information, patients with high NXT1 expression had a significantly worse prognosis (Fig. 6).

#### Downregulation of NXT1 Suppressed the Migration and Invasion of Hepatocellular Carcinoma Cells

To validate NXT1 expression in HCC, NXT1 levels were evaluated in tumor tissues and adjacent normal samples. As illustrated in Fig. 7A-7C, the mRNA and protein levels of NXT1 were notably elevated in tumor tissues compared

to adjacent normal samples. Meanwhile, NXT1 levels were markedly increased in HCC cell lines, HCCLM3 and HepG2, when compared to THLE-2 cells, with HCCLM3 cells exhibiting the highest levels of NXT1 expression (Fig. 7D-7F).

Next, to explore the functional role of NXT1 in HCC cells, NXT1 gene expression was silenced through siRNA transfection. As demonstrated in Fig. 8A-8C, NXT1 siRNA1 notably reduced NXT1 mRNA and protein levels in HCCLM3 cells compared to the siRNA NC group. Meanwhile, NXT1 siRNA1 remarkably suppressed HCCLM3 cell viability, migration, and invasion compared to the siRNA NC group (Fig. 8D-8H). These results suggested that NXT1 may function as an oncogene in HCC.

#### DISCUSSION

NXT1 (nuclear transport factor 2-like export factor 1, also known as p15) encodes a protein located in the nuclear

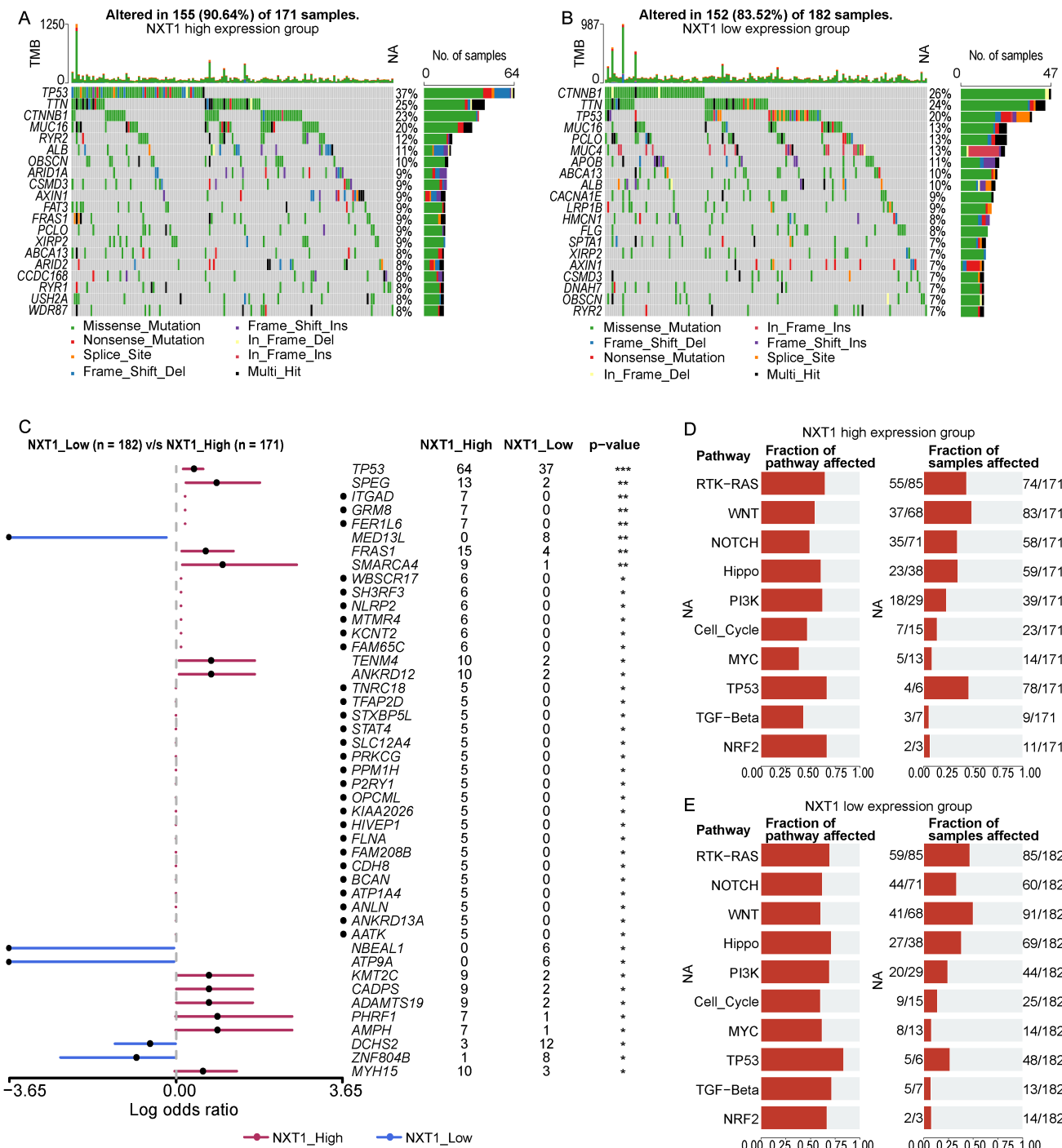


**Figure 3.** Mutation analysis in high and low NXT1 expression groups. (A-B) Mutation analysis in *NXT1<sup>high</sup>* group and *NXT1<sup>low</sup>* group. (C) Differences in mutation genes between *NXT1<sup>high</sup>* group and *NXT1<sup>low</sup>* group. (D-E) The ratios of gene mutation in 10 tumor-related pathways in *NXT1<sup>high</sup>* group and *NXT1<sup>low</sup>* group.

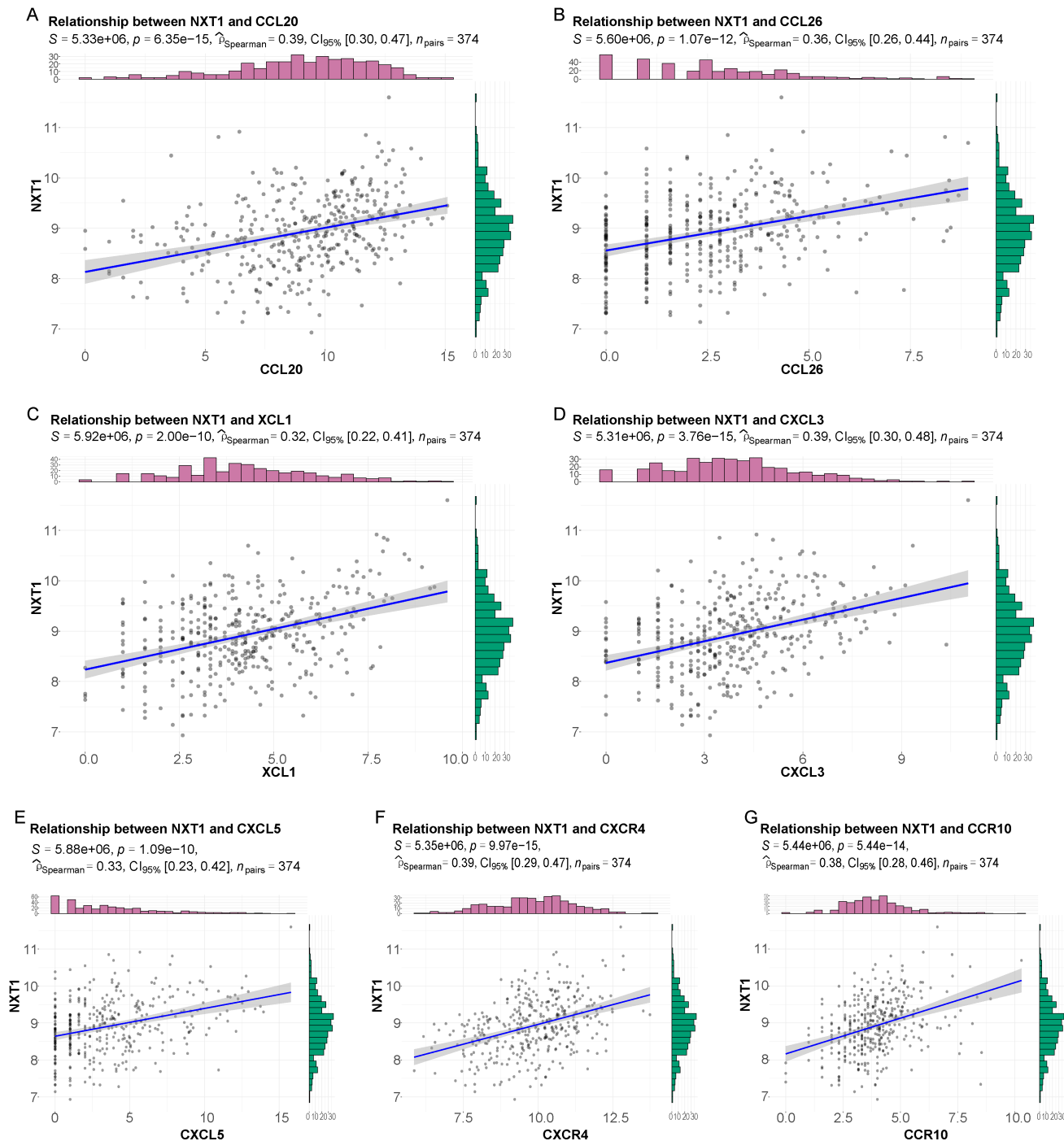


**Figure 4.** Relationship between NXT1 and chemokines/chemokine receptors. (A-G) Correlation analysis of NXT1 expression level and 7 most significant chemokines/chemokine receptors.

envelope, which plays a crucial role in the nuclear export of RNA molecules,<sup>18</sup> such as mRNAs, transfer RNAs (tRNAs), and small nuclear RNAs (snRNAs), from the nucleus to the cytoplasm. NXT1 has been identified as

a rapidly lethal factor in other diseases, such as MYCN-amplified neuroblastoma.<sup>19</sup> Additionally, NXT1 is essential for the nuclear export mediated by CRM1.<sup>20</sup> CRM1 has been shown to contribute to oncogenesis in various

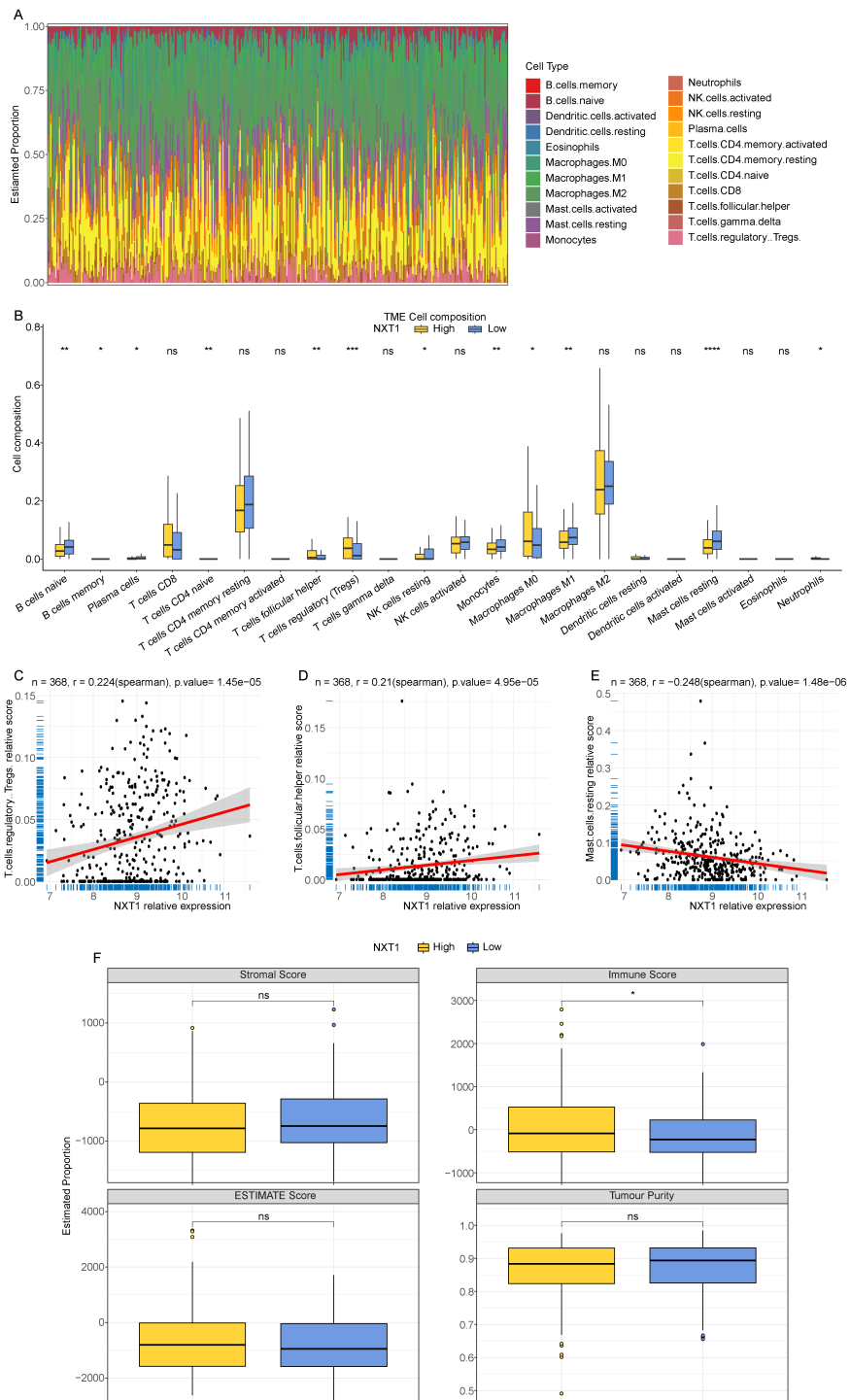


**Figure 5.** Immune infiltration analysis of hepatocellular carcinoma samples. (A) Relative abundance of 22 types of immune cells across all samples. (B) The infiltration ratios of 22 types of immune cells in the *NXT1*<sup>high</sup> group and the *NXT1*<sup>low</sup> group. (C-E) Correlation analysis between *NXT1* expression and Tregs, follicular helper T cells, and resting mast cells. (F) ImmuneScore, ESTIMATEScore, StromalScore, and TumorPurity in *NXT1*<sup>high</sup> group and *NXT1*<sup>low</sup> group.

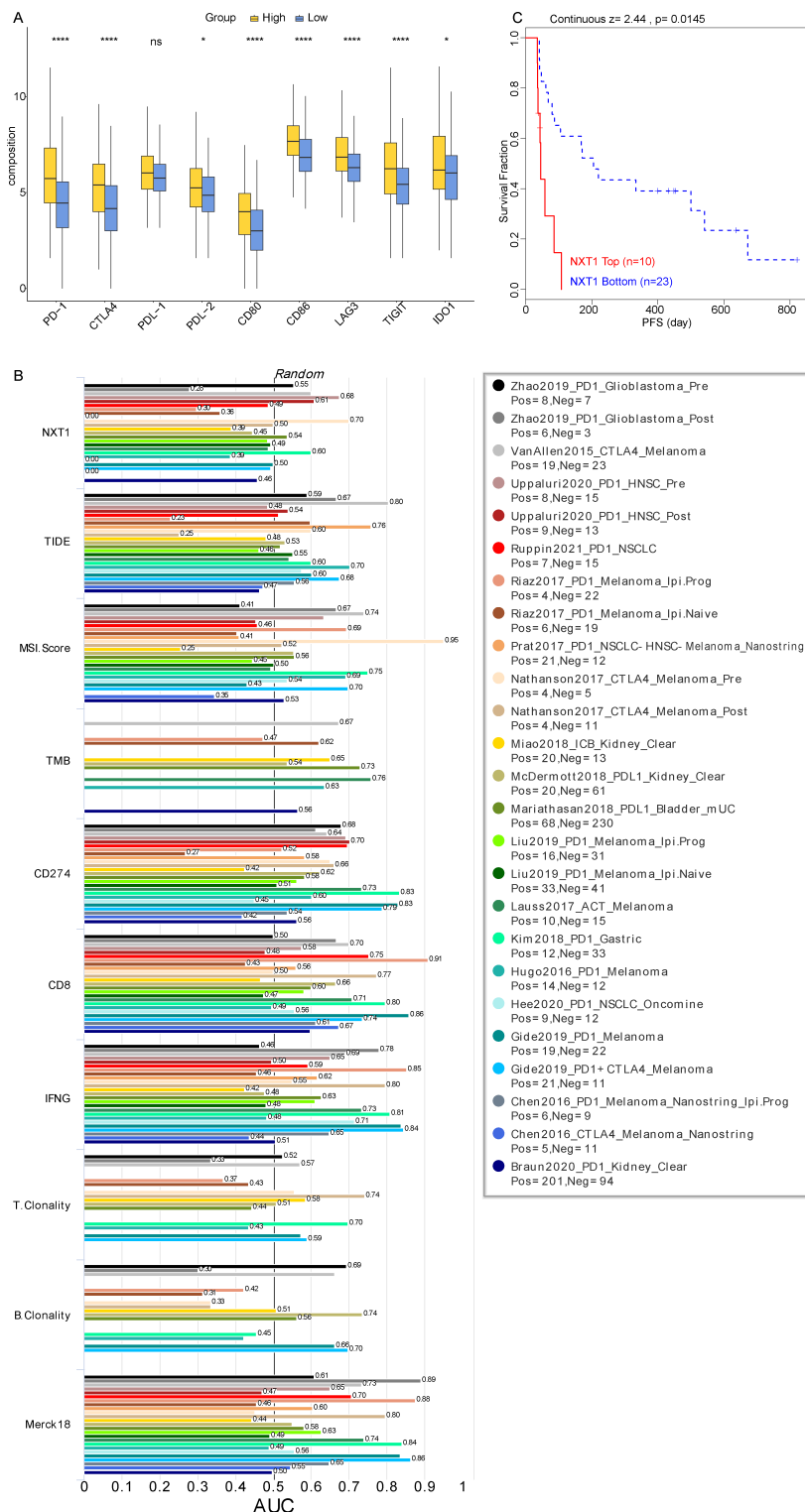


**Figure 6.** Analysis of immune therapy response and immune checkpoint expression. (A) Expression of 9 immune checkpoint genes in  $\text{NXT1}^{\text{high}}$  group and  $\text{NXT1}^{\text{low}}$  group. (B) Correlation of  $\text{NXT1}$  with standardized cancer immune evasion biomarkers in the ICB datasets. (C) KM survival curves of  $\text{NXT1}$  predicting ICB treatment in the Miao2018\_ICB dataset.

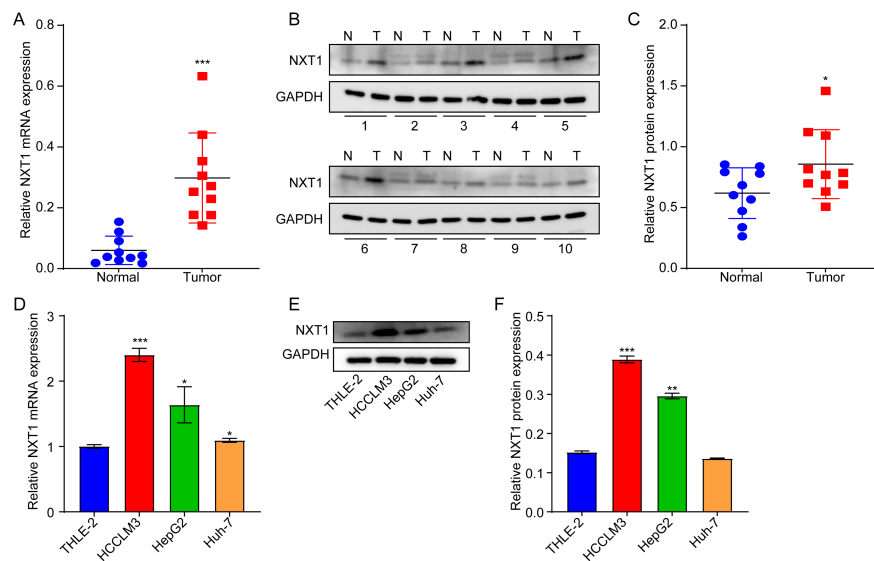


**Figure 7.** NXT1 expression is upregulated in hepatocellular carcinoma tissues and hepatocellular carcinoma cell lines. (A, B, C) RT-qPCR and western blot analyses of NXT1 levels in HCC tissues ( $n = 10$ ) and adjacent normal tissues ( $n = 10$ ). \* $P < .05$ , \*\* $P < .01$  vs Normal group. (D, E, F) RT-qPCR and western blot analyses of NXT1 levels in THLE-2, HCCLM3, HepG2, and Huh7 cells. \* $P < .05$ , \*\* $P < .01$ , \*\*\* $P < .001$  vs THLE-2 group.

cancers.<sup>21</sup> Inhibition of CRM1-mediated nuclear export has been demonstrated to enhance the accumulation of mTOR in the nucleus, resulting in decreased protein levels of mTOR and its downstream targets, STAT3 and MMP9, in ovarian cancer cells.<sup>22</sup> Similarly, the results indicated that downregulation of *NXT1* notably reduces HCC cell proliferation, migration, and invasion, suggesting that *NXT1* may function as an oncogene in HCC. However, the mechanisms by which *NXT1* regulates HCC progression remain poorly understood. Future studies are necessary to explore the molecular mechanisms underlying its function and to investigate whether *NXT1* exerts its oncogenic effects in HCC cells via a CRM1-dependent pathway.

Furthermore, the results demonstrated that *NXT1* may potentially act as a potential marker for predicting HCC prognosis. High levels of *NXT1* were associated with poor prognosis of HCC patients. Research has highlighted the crucial role of immune cell infiltration within the TME, demonstrating its close relationship with patient survival and prognosis.<sup>23</sup> In particular, the infiltration of M1 macrophages within tumor tissue correlates with a more favorable prognosis, whereas a high infiltration of M2 macrophages and Tregs within tumor tissue tends to correlate with worse prognosis of cancer patients.<sup>23,24</sup> The results align with these observations, revealing that, compared to the *NXT1*<sup>low</sup> group, patients in the *NXT1*<sup>high</sup> group exhibited increased infiltration of M0 macrophages and Tregs, along

with a notable decrease in M1 macrophage infiltration. These findings showed that elevated levels of *NXT1* contribute to poor prognostic outcomes in HCC patients, likely due in part to an imbalance of immune cell populations.

Treg cells represent a subset of immunosuppressive cells that inhibit the immune system's response to tumors and promote IE. Research has indicated that Tregs can be chemoattracted to the TME by specific chemokines, including CCL20 and CXCL5.<sup>25,26</sup> In a study conducted by Li et al,<sup>25</sup> it was demonstrated that DDR1/CXCL5 facilitates the creation of neutrophil extracellular traps, thereby enhancing the immune infiltration of Tregs, which promotes tumor growth and metastasis. Chen et al<sup>26</sup> discovered that the CCL20-CCR6 axis is responsible for the movement of circulating Tregs into the TME, consequently contributing to disease progression and unfavorable outcomes in HCC patients. The findings indicate a positive correlation between *NXT1* expression and the levels of CXCL5 and CCL20 in HCC. Given this information, it was proposed that *NXT1* may enhance the infiltration of Tregs into the TME by influencing chemokines and their receptors. This mechanism may promote IE, ultimately leading to a worse prognosis in HCC. However, this hypothesis requires further validation in future studies.

Genetic mutations are closely linked to the progression of cancer.<sup>27</sup> For example, *TP53*, a key tumor suppressor,

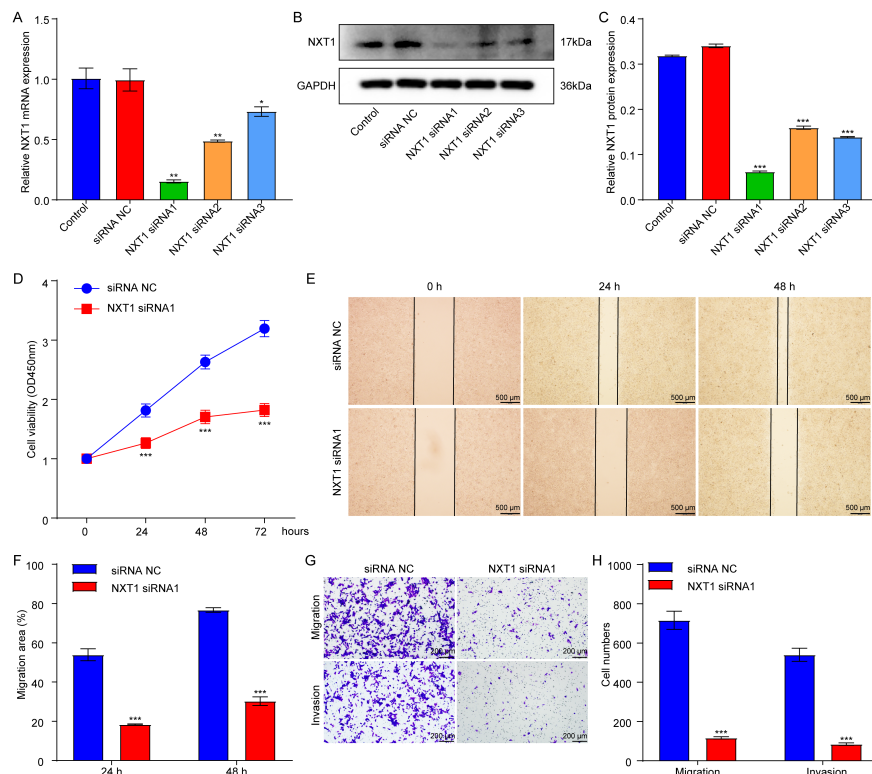


**Figure 8.** Downregulation of *NXT1* suppressed the migration and invasion of hepatocellular carcinoma cells. (A, B, C) HCCLM3 cells were transfected with siRNA NC, *NXT1* siRNA1, *NXT1* siRNA2, and *NXT1* siRNA3. Reverse transcription quantitative polymerase chain reaction and western blot assays were applied to assess *NXT1* mRNA and protein levels in transfected HCCLM3 cells. (D) HCCLM3 cells were transfected with siRNA NC and *NXT1* siRNA1. CCK-8 assay was conducted to evaluate cell viability. (E, F) Wound healing assay was employed to determine cell migration. (G, H) Transwell assay was conducted to assess cell migration and invasion. \**P* < .05, \*\**P* < .01, \*\*\**P* < .01 vs siRNA NC group.

is frequently mutated in human cancers, rendering its alteration a carcinogenic factor.<sup>27</sup> To gain deeper insights into the influence of *NXT1* on the progression and prognosis of HCC, the mutation status of genes in the *NXT1*<sup>high</sup> and *NXT1*<sup>low</sup> groups was analyzed. The results showed that mutations in the *TP53* gene are the most common in both groups, with a higher mutation rate observed in the *NXT1*<sup>high</sup> group compared to the *NXT1*<sup>low</sup> group. These findings showed that elevated expression of *NXT1* correlates with more frequent *TP53* mutations in HCC, implying a potential link between *TP53* mutation and *NXT1* levels in HCC progression, which warrants further investigation in future research.

To summarize, this research for the initial time demonstrated that elevated *NXT1* expression is linked to an unfavorable prognosis and correlates with the presence of various immune cell types and levels of immune checkpoints. Additionally, the results also found that downregulation of *NXT1* notably suppresses HCC cell viability, migration, and invasion, suggesting the oncogenic roles of

*NXT1* in HCC. These results imply that *NXT1* may serve as a prognostic marker and a potential therapeutic target for HCC.

Furthermore, there are some limitations in this article. The rates of incidence and mortality for HCC differ significantly among various geographic and ethnic groups. Further research is required to determine whether geographical and ethnic differences can influence the ability of *NXT1* to predict the prognosis of HCC patients, as well as investigate whether *NXT1* can serve as an independent risk factor for HCC patients. Moreover, the molecular mechanism by which *NXT1* exerts its oncogenic effects in HCC warrants comprehensive investigation in future studies. Meanwhile, the anti-tumor effect of *NXT1* deficiency in HCC was explored in vitro; however, the function of *NXT1* in HCC in vivo remains unexamined and requires further investigation. Furthermore, the results showed that HCC patients in the *NXT1*<sup>high</sup> group exhibited higher levels of 8 immune checkpoints than that in the *NXT1*<sup>low</sup> group, indicating that they might

be more likely to benefit from immunotherapy. It has been demonstrated that hepatitis B virus (HBV), hepatitis C virus (HCV), and nonalcoholic fatty liver disease (NAFLD) are well-established as the predominant etiological drivers of HCC.<sup>28,29</sup> Clinical evidence indicates that HCC patients with different underlying etiologies exhibit distinct responses to ICI therapy.<sup>30</sup> Patients with HBV-related HCC may benefit more from ICI treatment compared to those with HCV-related HCC.<sup>30</sup> While these observations suggest a critical role for disease etiology in influencing treatment outcomes, the potential involvement of NXT1 in this context remains unexplored. Unfortunately, the public databases utilized in this research did not provide clinical annotations of HCC etiologies such as HBV/HCV infection or NAFLD. Consequently, stratifying patients based on their underlying causative factors was not possible, which hindered the evaluation of whether NXT1 expression differentially influences prognosis or ICI treatment responses across these etiological subgroups. Future studies incorporating well-annotated, etiology-stratified cohorts will be essential to address this question.

**Data Availability Statement:** The data that support the findings of this study are available in The Cancer Genome Atlas (TCGA, <https://tcga-data.nci.nih.gov/tcga/>) database, the International Cancer Genome Consortium (ICGC, <https://dcc.icgc.org/>) and the Gene Expression Omnibus (GEO, <https://www.ncbi.nlm.nih.gov/geo/>) database.

**Ethics Committee Approval:** Ethical committee approval was received from the Ethics Committee of University of Shanxi Provincial Cancer Hospital / Shanxi Hospital Cancer Hospital of Chinese Academy of Medical Sciences (approval number: KY2024010; date: January 6, 2024).

**Informed Consent:** Written informed consent was obtained from the patients who agreed to take part in the study.

**Peer-review:** Externally peer-reviewed.

**Author Contributions:** Concept – Y.C., L.L., Y.P., X.J., Y.C., F.W., Q.Z.; Design – Y.C., L.L., Y.P., X.J., Y.C., F.W., Q.Z.; Supervision – Q.Z., F.W.; Resources – Y.C., F.W., Q.Z.; Materials – Q.Z., F.W., Y.P.; Data Collection and/or Processing – Y.P., C.L., M.L., W.L., M.Z.; Analysis and/or Interpretation – Y.P., C.L.; Literature Search – F.W., Q.Z.; Writing Manuscript – M.L., M.Z.; Critical Review – Y.P., X.J., L.L., Y.C., F.W., Q.Z.

**Declaration of Interests:** The authors have no conflicts of interest to declare.

**Funding:** This study was supported by Beijing Municipal Administration of Hospitals Incubating Program (Grant No. PX2020068 & PX2019063).

## REFERENCES

- Bray F, Laversanne M, Sung H, et al. Global cancer statistics 2022: GLOBOCAN estimates of incidence and mortality worldwide for 36 cancers in 185 countries. *CA Cancer J Clin.* 2024;74(3):229-263. [\[CrossRef\]](#)
- Crocetti L, Scalise P, Bozzi E, Candita G, Cioni R. Thermal ablation of hepatocellular carcinoma. *J Med Imaging Radiat Oncol.* 2023;67(8):817-831. [\[CrossRef\]](#)
- Zhao H, Ling Y, He J, et al. Potential targets and therapeutics for cancer stem cell-based therapy against drug resistance in hepatocellular carcinoma. *Drug Resist Updat.* 2024;74:101084. [\[CrossRef\]](#)
- Liu G, Shi A, Wang N, et al. Polyphenolic proanthocyanidin-B2 suppresses proliferation of liver cancer cells and hepatocellular carcinogenesis through directly binding and inhibiting AKT activity. *Redox Biol.* 2020;37:101701. [\[CrossRef\]](#)
- Lichterman JN, Reddy SM. Mast cells: A new frontier for cancer immunotherapy. *Cells.* 2021;10(6):1270. [\[CrossRef\]](#)
- Marzi L, Mega A, Gitto S, Pelizzaro F, Seeber A, Spizzo G. Impact and novel perspective of immune checkpoint inhibitors in patients with early and intermediate stage HCC. *Cancers.* 2022;14(14):3332. [\[CrossRef\]](#)
- Kelley RK, Sangro B, Harris W, et al. Safety, efficacy, and pharmacodynamics of tremelimumab plus durvalumab for patients with unresectable hepatocellular carcinoma: randomized expansion of a Phase I/II study. *J Clin Oncol.* 2021;39(27):2991-3001. [\[CrossRef\]](#)
- Xie QK, Zhao YJ, Pan T, et al. Programmed death ligand 1 as an indicator of pre-existing adaptive immune responses in human hepatocellular carcinoma. *Oncoimmunology.* 2016;5(7):e1181252. [\[CrossRef\]](#)
- Wildes TJ, Dyson KA, Francis C, et al. Immune escape after adoptive T-cell therapy for malignant gliomas. *Clin Cancer Res.* 2020;26(21):5689-5700. [\[CrossRef\]](#)
- Lu C, Klement JD, Smith AD, et al. p50 suppresses cytotoxic T lymphocyte effector function to regulate tumor immune escape and response to immunotherapy. *J Immunother Cancer.* 2020;8(2):e001365. [\[CrossRef\]](#)
- Peng L, Pan B, Zhang X, et al. Lipopolysaccharide facilitates immune escape of hepatocellular carcinoma cells via m6A modification of lncRNA MIR155HG to upregulate PD-L1 expression. *Cell Biol Toxicol.* 2022;38(6):1159-1173. [\[CrossRef\]](#)
- Ricciardi M, Zanotto M, Malpeli G, et al. Epithelial-to-mesenchymal transition (EMT) induced by inflammatory priming elicits mesenchymal stromal cell-like immune-modulatory properties in cancer cells. *Br J Cancer.* 2015;112(6):1067-1075. [\[CrossRef\]](#)
- Wang F, Zheng A, Zhang D, et al. Molecular profiling of core immune-escape genes highlights LCK as an immune-related prognostic biomarker in melanoma. *Front Immunol.* 2022;13:1024931. [\[CrossRef\]](#)
- Lawson KA, Sousa CM, Zhang X, et al. Functional genomic landscape of cancer-intrinsic evasion of killing by T cells. *Nature.* 2020;586(7827):120-126. [\[CrossRef\]](#)
- Ritchie ME, Phipson B, Wu D, et al. limma powers differential expression analyses for RNA-sequencing and microarray studies. *Nucleic Acids Res.* 2015;43(7):e47. [\[CrossRef\]](#)
- Yu G, Wang LG, Han Y, He QY. clusterProfiler: an R package for comparing biological themes among gene clusters. *OMICS.* 2012;16(5):284-287. [\[CrossRef\]](#)
- Newman AM, Liu CL, Green MR, et al. Robust enumeration of cell subsets from tissue expression profiles. *Nat Methods.* 2015;12(5):453-457. [\[CrossRef\]](#)

18. Aibara S, Katahira J, Valkov E, Stewart M. The principal mRNA nuclear export factor NXF1:NXT1 forms a symmetric binding platform that facilitates export of retroviral CTE-RNA. *Nucleic Acids Res.* 2015;43(3):1883-1893. [\[CrossRef\]](#)

19. Malone CF, Dharia NV, Kugener G, et al. Selective modulation of a pan-essential protein as a therapeutic strategy in cancer. *Cancer Discov.* 2021;11(9):2282-2299. [\[CrossRef\]](#)

20. Black BE, Holaska JM, Lévesque L, et al. NXT1 is necessary for the terminal step of Crm1-mediated nuclear export. *J Cell Biol.* 2001;152(1):141-155. [\[CrossRef\]](#)

21. Ferreira Bl, Cautain B, Grenho I, Link W. Small molecule inhibitors of CRM1. *Front Pharmacol.* 2020;11:625. [\[CrossRef\]](#)

22. Shao WY, Yang YL, Yan H, Huang Q, Liu KJ, Zhang S. Phenethyl isothiocyanate suppresses the metastasis of ovarian cancer associated with the inhibition of CRM1-mediated nuclear export and mTOR-STAT3 pathway. *Cancer Biol Ther.* 2017;18(1):26-35. [\[CrossRef\]](#)

23. Ruiz-Ranz M, Lequerica-Fernández P, Rodríguez-Santamaría T, et al. Prognostic implications of preoperative systemic inflammatory markers in oral squamous cell carcinoma, and correlations with the local immune tumor microenvironment. *Front Immunol.* 2022;13:941351. [\[CrossRef\]](#)

24. Ohue Y, Nishikawa H. Regulatory T (Treg) cells in cancer: can Treg cells be a new therapeutic target? *Cancer Sci.* 2019;110(7):2080-2089. [\[CrossRef\]](#)

25. Li H, Li J, Bai Z, Yan S, Li J. Collagen-induced DDR1 upregulates CXCL5 to promote neutrophil extracellular traps formation and Treg infiltration in breast cancer. *Int Immunopharmacol.* 2023;120:110235. [\[CrossRef\]](#)

26. Chen KJ, Lin SZ, Zhou L, et al. Selective recruitment of regulatory T cell through CCR6-CCL20 in hepatocellular carcinoma fosters tumor progression and predicts poor prognosis. *PLoS One.* 2011;6(9):e24671. [\[CrossRef\]](#)

27. Deng S, Lu X, Zhang Z, Meng R, Li M, Xia S. Identification and assessment of PLK1/2/3/4 in lung adenocarcinoma and lung squamous cell carcinoma: evidence from methylation profile. *J Cell Mol Med.* 2021;25(14):6652-6663. [\[CrossRef\]](#)

28. Polyzos SA, Chrysavgis L, Vachliotis ID, Chartampilas E, Cholongitas E. Nonalcoholic fatty liver disease and hepatocellular carcinoma: insights in epidemiology, pathogenesis, imaging, prevention and therapy. *Semin Cancer Biol.* 2023;93:20-35. [\[CrossRef\]](#)

29. Sun Y, Zhang H, Long J, Zhang Y, Zheng J, Yuan C. Percutaneous thermal ablation combined with transcatheter arterial chemoembolization for hepatitis C virus-related hepatocellular carcinoma: efficacy and survival. *Front Oncol.* 2022;12:978614. [\[CrossRef\]](#)

30. Du Q, Yuan J, Ren Z. Hepatocellular carcinoma patients with hepatitis B virus infection exhibited favorable survival from immune checkpoint inhibitors: A systematic review and meta-analysis. *Liver Cancer.* 2024;13(4):344-354. [\[CrossRef\]](#)

**Supplementary Table 1.** Immune escape related genes used in this study.

Gene Symbol	Pigs	Det1	Pced1b
B2m	Pigu	Dicer1	Pdcd6ip
Ifngr1	Ppp2r2a	Dnajc13	Pdss2
Jak2	Psmb8	Dot1l	Pi4kb
Socs1	Rb1cc1	Dph5	Pigk
Tap1	Rbm15	Eif3h	Pigt
Tap2	Ric8	Emc2	Pkn2
Tapbp	Rnf31	Emc3	Ppp1ca
Adar	Scaf4	Emc4	Ppp1r8
Atg10	Smg7	Emc6	Ppp2r3c
Atg101	Tab1	F8a	Prkcsb
Cflar	Tab2	Fam58b	Psmb9
Fitm2	Tmem127	Fas	Psmg1
Gpaa1	Tnfrsf1b	Fntb	Ptar1
Gpi1	Ube2g2	Gale	Rce1
Ifngr2	Ube2n	Gls	Rgp1
Ikbkg	Vdac2	H2-K1	Ric1
Irf1	Vps29	Hcfc2	S100ppb
Jak1	Vps35	Hdgfrp2	Sarnp
Otud5	Vps4b	Hexim1	Setd1a
Ptpn2	Wipi2	Hira	Setdb1
Rbck1	Zcchc14	Hspa13	Slc25a32
Stat1	Acad9	Ifnar1	Spcs1
Stat2	Actb	Ifnar2	Srrt
Tnfaip3	Ago2	Ikbkb	Srsf7
Tnfrsf1a	Ahsa1	Ino80	Stoml2
Traf2	Anapc15	Ippk	Susd6
Atg12	Arf6	Irf9	Tbk1
Atg3	Atg14	Jagn1	Tfrc
Atg5	Atg7	Jmjd6	Tgfb2r
Becn1	Atg9a	Kat6a	Tmem208
Chic2	Atp13a1	Klf16	Tradd
Dnttip1	Atxn7l3	Kmt2a	Trpm7
Emc8	BC003331	Lipt2	Ubr5
Erap1	Bcl2l1	Mapk1	Ufc1
Erp44	Bola3	Med16	Ufl1
Fadd	Brat1	Med23	Usp7
Hdac1	Brpf1	Med24	Uxs1
Ist1	Cad	Mgat1	Vps13a
Map3k7	Calr	Mta2	Vps16
Men1	Cep55	N6amt1	Wdr7
Mogs	Chmp5	Ncbp1	Wdr83
Ndufa13	Cox6c	Ndufaf6	Wwp2
Nxt1	Crebbp	Nploc4	Yap1
Otulin	Cul3	Nup188	Zc3h3
Pdia3	Dcp1a	Pcbp2	

**Supplementary Table 2.** The clinical information of HCC patients.

No.	Age	Gender	Tumor Size (cm×cm)	T	N	M	Clinical stage	Etiology (Alcohol, HBV, HCV, others)
1	55	Male	5.3×4.7	2	0	0	II	HBV
2	61	Male	15×11.5	3	0	0	IIIA	HBV
3	73	Male	2.5×2.0	2	0	0	II	HCV
4	70	Male	1.5×1.5	2	0	0	II	HBV
5	78	Male	9.7×9.0	4	0	0	IIIB	Alcohol
6	67	Female	5.0×4.5	2	0	0	II	No
7	59	Male	3.5×2.2	2	0	0	II	Alcohol
8	55	Male	3.5×3.0	1b	0	0	I	HBV
9	67	Female	7.0×6.5	2	0	0	II	HBV
10	66	Female	2.6×2.9	2	0	0	II	HBV

HBV, hepatitis B virus; HCV, hepatitis C virus.

**Supplementary Table 3.** Primer sequences for qPCR.

Genes	Forward Primer (5'-3')	Reverse Primer (5'-3')
Nuclear Transport Factor 2 Like Export Factor 1 (NXT1)	CTTCCAGCGAGTTCCAAATCA	CAGATGACAACAAGGACCGTG
Glyceraldehyde-3-Phosphate Dehydrogenase (GAPDH)	GAAGGTGAAGGTCGGAGTC	GAAGATGGTGTGGGATTTC

**Supplementary Table 4.** siRNA sequences.

Genes	Sequences (5'-3')	
Nuclear Transport Factor 2 Like Export Factor 1 (NXT1) siRNA1	sense	GAUCGCAAGUGACUGCUUC
	antisense	GAAGCAGUCACUUGCGAUC
NXT1 siRNA2	sense	CCUCGACUCUCAAGGAUGU
	antisense	ACAUCCUUGAGAGUCGAGG
NXT1 siRNA3	sense	GCGAGUUCCAAAUCAGCGU
	antisense	ACGCUGAUUUGGAACUCGC
Negative control	sense	UUCUCCGAACGUGUCACGU
	antisense	ACGUGACACGUUCGGAGAA

**Supplementary Table 5.** Gene Ontology (GO) enrichment analysis.

[https://docs.google.com/spreadsheets/d/1asVV7t8WCwZ\\_ZeJxLgwaPZtxjzis\\_KIK4Cr9-IKdIUU/edit?usp=sharing](https://docs.google.com/spreadsheets/d/1asVV7t8WCwZ_ZeJxLgwaPZtxjzis_KIK4Cr9-IKdIUU/edit?usp=sharing)

**Supplementary Table 6.** Kyoto Encyclopedia of Genes and Genomes (KEGG) enrichment analysis.

ID	Description	BgRatio	pvalue	p.adjust	qvalue	genelD	Count
hsa05169	Epstein-Barr virus infection	202/8292	0.0002699	0.0040826	0.0029952	TAP2/TRADD/TAPBP	3
hsa05170	Human immunodeficiency virus 1 infection	212/8292	0.0003113	0.0040826	0.0029952	TAP2/TRADD/TAPBP	3
hsa05163	Human cytomegalovirus infection	225/8292	0.0003711	0.0040826	0.0029952	TAP2/TRADD/TAPBP	3
hsa04612	Antigen processing and presentation	78/8292	0.0012787	0.0105493	0.0077395	TAP2/TAPBP	2
hsa05164	Influenza A	171/8292	0.0060056	0.0396371	0.0290798	NXT1/TRADD	2
hsa00563	Glycosylphosphatidylinositol (GPI)-anchor biosynthesis	26/8292	0.018672	0.1026962	0.0753433	PIGT	1
hsa05340	Primary immunodeficiency	38/8292	0.0271914	0.120401	0.0883325	TAP2	1
hsa02010	ABC transporters	45/8292	0.0321325	0.120401	0.0883325	TAP2	1
hsa03050	Proteasome	46/8292	0.0328366	0.120401	0.0883325	PSMB9	1
hsa04920	Adipocytokine signaling pathway	69/8292	0.0489149	0.1509072	0.1107134	TRADD	1